Journal of Fluorescence, Vol. 2, No. 2, 1992

Wavelength-Dependent Rotation of Dye Molecules in a Polar Solution

D. M. Gakamsky,[1] N. A. Nemkovich,[1] and A. N. Rubinov[1]

Received November 15, 1991; revised June 19, 1992; accepted June 26, 1992

Investigation of rotation movement of 3-amino-*N*-methylphthalimide in glycerol was carried out, taking into consideration the fluctuation of solvate structure. It was shown theoretically and experimentally that structural relaxation of the solvate shell, which follows excitation of the dye molecule, causes not only shift of the fluorescence spectrum in time but also additional rotation of the dye molecule. This effect, which may be called "wavelength-dependent rotation," depends on the light frequency of both excitation and fluorescence. In particular, at excitation near the maximum of the absorption band, when the relaxation process is followed with the red shift of the fluorescence maximum, the anisotropy of fluorescence decreases faster in the red part of the fluorescence band than in the blue part. On the contrary, in the case of far anti-Stokes excitation, when the temporal shift of fluorescence is going to the blue, the anisotropy in the red part of the spectrum drops more slowly than in the blue part. Finally, there is a special excitation frequency which causes neither change of the fluorescence maximum nor acceleration of the rotational movement of the dye molecule. It is also shown that the temporal evolution of the spectrum and anisotropy of fluorescence in a polar dye solution may be quantitatively described using the so-called inhomogeneous broadening function (IBF). This function gives the distribution of dye molecules in a solution over frequencies of pure electronic transition due to fluctuations of the surrounding shell structure. Measurements of IBF changes in time carried out for 3-amino-*N*-methylphthalimide showed that during first 3 ns after excitation, the half-width of the IBF grows, and at the same time its maximum quickly shifts to the red. At the later time period there are only small changes of IBF position but considerable exponential decrease in its half-width. The IBF during this period preserves the Gaussian shape.

KEY WORDS: Inhomogeneous broadening; solvate; kinetic spectroscopy; kinetics of fluorescence anisotropy; intermolecular relaxation; continuum model.

INTRODUCTION

The recent years have seen great interest in time-resolved spectroscopy of dye solutions, particularly due to the wide application of the fluorescent probe method in biophysics [1]. The use of dye molecules as probe is based on the strong dependence of their electronic spectra on the potential of intermolecular interactions. The additional interest in this problem is focused on the important role which molecular dynamics of solvatation play in reactions of charge transfer in polar solutions [2–5].

Electronic spectra of polar dye solutions are known [6] to be inhomogeneously broadened. The model of several discrete states fails to describe the kinetics of fluorescence and relaxation of time-resolved spectra of this molecular system. Bakhshiev and Mazurenko [7] proposed another model for describing the kinetic behavior of the solvent relaxation of polar dye solutions.

[1] Institute of Physics, Belarusian Academy of Sciences, Francisk Skorina Ave. 70, 220602 Minsk, Belarus.

1053-0509/92/0600-0081$06.50/0

In this model, the fluorescence kinetics is represented as the product of the decay function describing the fluorescent level decay (without taking into account the relaxation) and of the time-resolved spectrum, which is smoothly shifting with time in the frequency scale without changing its shape. To associate the character of the shift of the time-resolved fluorescence spectrum with the microcharacteristics of the solution, representations of the physics of dielectrics based on the Onsager-Bottcher and Debye models are often used [8–15]. However, there is a number of works in which a molecular theory of solvation dynamics is developed [16,17].

In [18], the continuum model [7] was used to describe the nonexponential fluorescence kinetics in polar solutions. It turned out that for a good quantitative description of experimental kinetics, the decay function should be given as the two-exponential one. Such a complicated character of the decay function would mean that the probability of radiative transition changes in the process of relaxation. This change, though not completely improbable, looks like an artificial assumption, which does not always take place. The experimental data are available only for phthalimide derivatives [19]. For these substances it was shown that the excited-state lifetime in solid polar solutions is independent of the frequency of the pure electronic transition. In other words, in this case the probability of the optical S_0–S_1 transition does not depend on the solvate surrounding of the chromofore. In the present paper, another approach for describing the fluorescence kinetics and time-dependent fluorescence shift (TDFS) from the point of view of a continuum model is proposed. While describing the fluorescence kinetics and TDFS of polar solutions, we took into consideration inhomogeneous broadening of its electronic spectra, i.e., the continuous distribution of individual fluorescent centers over the frequencies of pure electronic transitions. In this case the time-resolved fluorescent spectra are represented by convolution of the homogeneous spectrum and inhomogeneous broadening function (IBF), which changes its position in the frequency scale and shape during relaxation. In this case the quantitative description of experimental data is achieved using the monoexponential decay function.

The rotary motion of the fluorofore in a polar dye solution is often considered in terms of the generally accepted Einstein-Debye-Stokes theory [20]. In this theory it is not taken into account that the elementary system responsible for the spectral properties of solution (the fluorofore molecule and its environment) experiences intermolecular relaxation in the process of fluorescence. Since the energy of the dipole–dipole interactions responsible for the solvate deviation from equilibrium in polar liquids can be significantly higher than the energy of the thermal motion of molecules, a rotary motion in such a system cannot be described by the time-independent rotational diffusion constant [21].

The nonexponential fluorescence anisotropy kinetics in viscous solutions of phthalimide derivatives was first reported by us [22]. To interpret these results, we have used the model of forced rotations proposed in Ref. 23. The main points of the model are as follows. The direction of the electric dipole moment of the fluorofore on optical excitation can change. Since the dipole moment direction changes much faster than the reorientation of molecules in solvate takes place, the fluorofore must be affected by the moment of forces, tending to turn it to the reactive field direction. The possibility of such a process is also discussed in Ref. 13.

In the literature, there are other viewpoints, too, on the way the intermolecular relaxation caused by dipole–dipole interactions can influence fluorescence anisotropy kinetics. Lakowicz [24] assumes that, since in the process of intermolecular relaxation, the energy of the fluorofore interaction with the environment increases, this must lead to a slowing down of rotational diffusion in the course of spectral relaxation.

Another mechanism is proposed by Maroncelli and Fleming [13]; who discuss the fast component observed in the kinetics of emission anisotropy of coumarin-153 in polar solvents. In the authors opinion, this fast component can be associated with the rotation of the transition dipole moment during intermolecular relaxation.

The present paper considers the relationship between the character of spectral relaxation and the previously reported [25] dependence of the fluorescence anisotropy kinetics on the excitation and detection frequency. To explain the fast component of the fluorescence anisotropy, we used a more general model than the model of forced rotation [23]. We believe that the accelerated rotation of the fluorofore during spectral relaxation can also take place when the dipole moments in the ground and excited states have the same direction but differ in value.

According to the proposed model, rotation of the fluorofore molecule becomes faster during intermolecular relaxation due to the transformation of the configurational interaction free energy to the kinetic energy of intermolecular motion. As a particular case, this mechanism includes also the forced rotation of the fluorofore in the solvate field discussed above, since this rotation forms part of the process of configurational relaxation.

THE MODEL OF A POLAR SOLUTION

Recently, several theoretical models [2, 5, 16, 17, 26, 27] on the dynamics of solvation of a dye in a polar liquid have been carried out that take into account the molecular structure of the solvent. Calef and Wolynes [2] proposed a Smoluchowski-Vlasov equation for solvation dynamics. Fried and Mukamel [26] developed a microscopic theory, which incorporates non-Debye dielectric relaxation and solvate shell structure. The most commonly applied microscopic theory of solvation is the dynamical mean spherical approximation (MSA), which was proposed by Wolynes [16] and extended in Refs. 5 and 27. Unfortunately the microscopic theories of solvation do not take into account the inhomogeneous broadening of electronic spectra of dye in solutions due to the thermal motion of molecules in a liquid.

In Ref. 28 a model of solution with inhomogeneously broadened electronic spectra is considered in which the solvate state is described by the action of two forces. The first one is a polarizing force caused by a constant dipole moment μ in the fluorofore molecule which induces the reactive field R inside the solvate. The second is a returning force caused by the solvent molecule's interaction, which tends to return the solvate to the state with the zero reactive field. The deviation of the solvate configuration from equilibrium leads to an increase in its free energy compared to the minimum value in the equilibrium state. It is easy to see that this increase equals the work dA done by dipole μ on the reconstruction of solvate from the equilibrium state to the state mentioned above with a fluctuationally deviated configuration.

In the differential form, the work done by the rigid dipole μ on environment polarization, which leads to the increase in the reactive field by the value dR, is

$$dA = \mu dR \tag{1}$$

If we assume that the returning force is proportional to the reactive field, the free energy of ground-state solvate will be described by the following equation:

$$F_g(R) = (R - R_g^{eq})^2/2x \tag{2}$$

where R_g^{eq} is the reactive field in equilibrium solvate, and x is the solvent polarizability determined by the Clausius-Mossotti formula:

$$x = 2(\epsilon - 1)/a^3(2\epsilon + 1) \tag{3}$$

Here ϵ is the dielectric constant of the solvent, and a is the Onsager sphere radius.

The excited solvate free energy is determined by a similar relation:

$$F_e(R) = (R - R_e^{eq})^2/2x + h\nu_o + x(\mu_e + \mu_g)(\mu_e - \mu_g)/2 \tag{4}$$

where ν_o is the frequency of the pure electronic transition of the free-dye molecule, h is Plank's constant, μ_g and μ_e are the electric dipole moments of the dye molecule in the ground and excited states, and $R_e^{eq}$is the reactive field corresponding to the equilibrium excited state of the solvate.

The diagram of the solvate energy levels constructed according to Eqs. (2) and (4) (field diagram) is given in Fig. 1. It describes the dependence of the solvate free energy on the reactive field magnitude (the vibrational broadening of electronic levels is not shown in Fig. 1). The local solvate field R serves here as a generalized coordinate characterizing the state of the solvate. It changes due to the thermal fluctuation of the solution microstructure. Each point on the curves describing $F_g(R)$ and $F_e(R)$ corresponds to a particular type of solvate with the field R. Since the reactive field of

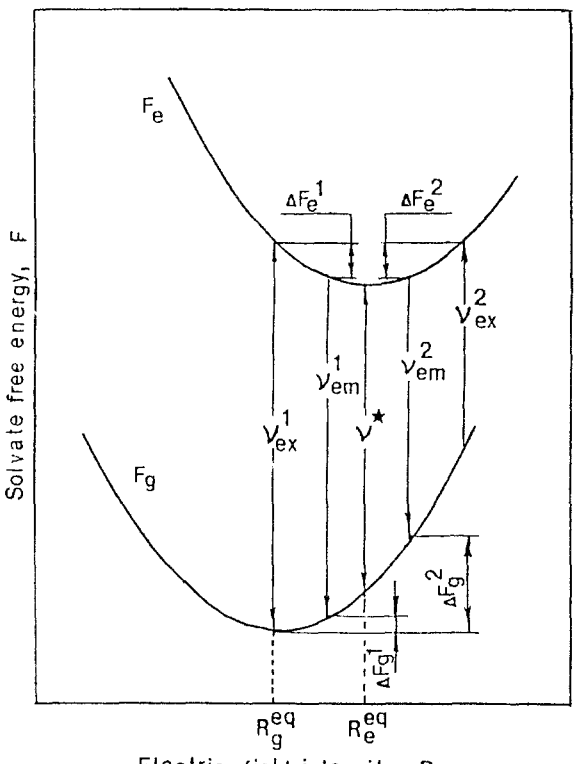

Fig. 1. The field diagram for 3ANMP in glycerol.

the solvate has no time to change during the electronic transition (except for its electronic component, which can be ignored), electronic transitions are represented in Fig. 1 by vertical arrows (intermolecular interpretation of the Frank-Condon principle).

Analysis of Fig. 1 shows that when the excitation frequency corresponds to ν_{ex}^1, the process of solvate relaxation is expected to be followed by the red shift of the fluorescence spectrum. On the contrary, if the excitation frequency is equal to ν_{ex}^2, the time-dependent shift of the spectrum will be to the blue region [29]. Between ν_{ex}^1 and ν_{ex}^2 there is a particular frequency ν^* at which, on excitation, the solvate at once appears in the equilibrium state, and therefore, the spectrum relaxation does not occur. An important result of this model is the Gaussian character of the equilibrium distribution of solvates over the frequencies of pure electronic transition for absorption (a) and emission (e):

$$\varphi_{a,e} = \frac{N_{a,e}(\nu)}{N_{a,e}} = \frac{1}{\sqrt{2\pi}\,\sigma} \exp\left[-\frac{(\nu - \nu_{a,e}^o)^2}{2\sigma^2}\right] \quad (5)$$

where $N_{a,e}(\nu)$ is the contribution of absorbing (emissing) solvate in which the pure electronic transition of the fluorofore is equal to ν, $N_{a,e}$ is the total concentration of absorbing (emissing) solvates,

$$\sigma = \frac{(\mu_e - \mu_g)}{h}\sqrt{xkT} \quad (6)$$

the frequency $\nu_{a,e}^o$ corresponding to the mean of the distribution is equal to ν_{ex}^1 for absorption and ν^* for fluorescence, k is the Boltzmann constant, and T is temperature. The Gaussian distribution of solvates over the frequencies of pure electronic transitions is the result of a Boltzmann distribution of solvate over the intermolecular interaction energy. Such an equilibrium distribution in the ground and excited states is established in the case when the lifetimes of both states are substantially longer than the characteristic time of molecular reorientation in the solvate.

EXPERIMENTAL

Kinetic measurements were made on a nanosecond laser spectrofluorimeter [30] which employed as an excitation source a distributed-feedback dye laser pumped by a TEA-nitrogen laser with a pulse duration of 1.8 ns. Fluorescence was measured by a photomultiplier ELU-18-FM (USSR) with a time resolution of about 1 ns and a stroboscopic detection system with signal preprocessing. Further processing of experimental data was done with an Electronika-60 computer.

The detection system provided measurement of four characteristics of fluorescence: the kinetics of fluorescence, the kinetics of the fluorescence anisotropy, time-resolved fluorescence spectra, and time-resolved fluorescence anisotropy spectra.

The spectral width of the slit in the recording monochromator was 3 nm. As the polarizer and analyzer, a Glan-Thompson prism and a Polaroid film were used. When measuring time-resolved fluorescence spectra, the polarizer was oriented at the magic angle.

The coefficients for correction of the spectral sensitivity of the detection system were determined by comparing the spectra of liquid solutions of reference substances when recorded on a standard SLM-4800 fluorimeter and on our setup. The photomultiplier spectral sensitivity maximum is in the region of 20,000 cm^{-1}, so that the correction coefficients within the spectral boundaries of detection (22,000–18,000 cm^{-1}) did not exceed the value of 3. The stationary absorption spectra were recorded on a Beckmann UV-5270 spectrophotometer.

3-Amino-*N*-methylphthalimide (3ANMP; Scheme I) was twice sublimed at T = 90°C and commercial glycerol was dried up and purified by vacuum distillation until the fluorescence of organic impurities became negligible compared with fluorescence of 3ANMP at a concentration of $5.0 \cdot 10^{-6}$ M. The glycerol solutions were stored in the dark and were protected from water absorption.

RESULTS AND DISCUSSION

Spectral Relaxation

There are several important works which have recently addressed the related topic of spectral inhomo-

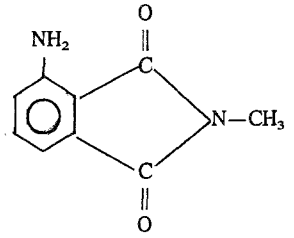

Scheme I

geneous broadening of complex organic compounds in solutions [6,28,29,31] and polymeric glasses [28,32–35].

The fluorescence kinetics of a viscous polar solution is known to be nonexponential [28,29]. However, its correct description by the models of two or three states is impossible, since time constants corresponding to the states turn out to be dependent on the recording wavelength [18].

According to the model [7], the kinetics of fluorescence $I(\nu,t)$ of the polar dye solution may be described by the following relation:

$$I(\nu,t) = i(t)\rho(\nu,t) \tag{7}$$

where the decay function $i(t) = I_o \exp(-t/\tau_{fl})$ [τ_{fl} is the excited-state lifetime, I_o is a constant, and $\rho(\nu,t)$ is a time-resolved fluorescence spectrum]. This model assumes that the time-resolved spectrum during the process of relaxation is smoothly shifting while its shape remains unaltered.

From the model of a polar solution, described above, it follows that the absorption and fluorescence spectra are determined by convolution of a corresponding inhomogeneous broadening function (IBF) and a homogeneous spectra:

$$\rho(\nu,t) = \int_o^\infty \varphi_{a,e}(\nu',t)\, S_{a,e}(\nu - \nu')d\nu' \tag{8}$$

where $\varphi_{a,e}(\nu',t)$ is a time-dependent IBF, and $S_{a,e}(\nu\text{-}\nu')$ is a homogeneous spectrum. Since the lifetime of a ground-state dye molecule is long, we can consider the solvate distribution over the frequencies of pure electronic transitions for absorption $\varphi_a(\nu)$ to be equilibrium and described by relation (5). The indices a and e refer to absorption and fluorescence, respectively.

As the homogeneous spectra $S_{a,e}(\nu)$, we used absorption and fluorescence spectra in a nonpolar solvent (hexane). The frequency of the pure electronic transition was determined from these spectra.

The calculation of IBF for 3ANMP ground-state absorption in glycerol by formula (8) (see Fig. 2) is hampered by the fact that the blue slope of the low-frequency absorption band (curve 1) is distorted by superposition with a second band. Therefore, the quality of calculation of stationary IBF (curve 4) can be correctly assessed in this case by comparing the experimental (curve 1) and calculated (curve 2) spectra only on their red slopes. Curve 3 in Fig. 2 corresponds to the homogeneous profile.

As a result, we have found that the IBF for absorption within the accuracy of the experiment is described by the Gaussian function with rms deviation σ = 700

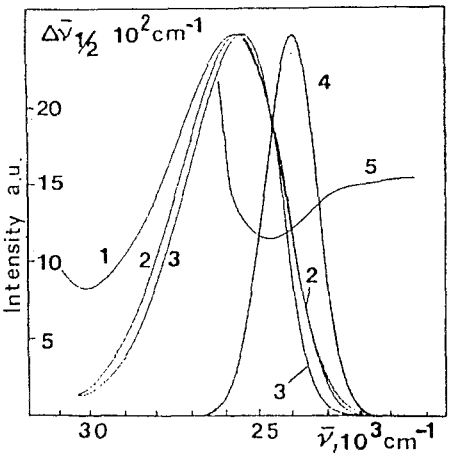

Fig. 2. The calculation of the IBF for the absorption and the dependencies of the IBF for fluorescence at the zero instant of time on the excitation frequency for 3ANMP solution in glycerol. (1) Stationary absorption spectrum; (2) calculated absorption spectrum; (3) homogeneous absorption spectrum; (4) IBF for absorption; (5) FWHM of IBF for fluorescence at the zero instant of time vs the excitation frequency.

cm^{-1} and its maximum is shifted relative to the pure electronic transition of the dye in a nonpolar solution by 1600 cm^{-1}. Now, knowing the IBF for absorption, we can easily calculate the IBF for fluorescence at the time moment immediately after excitation. At this moment of time, it is determined by the exciting light frequency.

Since the number of solvates with the 0–0 transition frequency at the zero instant of time in the excited state is equal to the product of the number of solvates in the ground state with the same frequency times the absorption coefficient of this type of solvate, the IBF at time $t=0$ is equal to [36]

$$\varphi_e(\nu,0) = \varphi_a(\nu)S_a(\nu - \nu_{ex}) \tag{9}$$

where ν_{ex} is the exciting light frequency.

The last relation permits calculation of the IBF half-width's dependence on the exciting light frequency (see Fig. 2, curve 5). It is seen from Fig. 2 that, due to the significant width of the homogeneous absorption spectrum in the excited state, a fairly wide distribution of solvates is always created. However, on the red slope there is a frequency range upon excitation in which quite noticeable selectivity of excitation is achieved. As shown in Ref. 28, the selectivity of excitation at the red slope of the absorption band is a fundamental feature of the dye solution. To calculate the IBF half-width at anti-Stokes excitation, the shape of the absorption band at a low-frequency wing was determined by the Stepanov

relation [37], since the spectra can be distorted by impurities when absorption in this region is measured.

The above method of determining IBF for the excited state is useful because it permits calculation of the time-resolved fluorescence spectrum at the zero moment of time when measurements were hampered because of the insufficient time resolution of the setup.

The IBF for an arbitrary instant of time can be determined from formula (8) if we use as $\rho_e(\nu,t)$ the time-resolved spectrum recorded at this instant of time. An example of calculation of the IBF for the instant of time 6 ns is given in Fig. 3 (curve 1). It turned out that, within the accuracy of the experiment, the shape of the IBF is close to Gaussian. Curve 3 in Fig. 3 corresponds to the homogeneous emission spectrum.

Figure 4 shows time-resolved fluorescence spectra (curves 1–3) and their corresponding IBFs (curves 4–6) for three instants of time—0, 3, and 6 ns. In Fig. 5a the points represent the correlation function $C(t) = [(\nu_e^0(t) - \nu_e^0(\infty)]/[(\nu_e^0(0) - \nu_e^0(\infty)]$, calculated from the mean of the IBF using Eq. (8). The point $C(t=0)$ was found from Eq. (9).

As it turned out, the observed dependence may be well described by the sum of two exponents:

$$\nu_e^0(t) = \nu_e^0(\infty) + \Delta\nu_f[\beta_1 \exp(t/\tau_1) + \beta_2 \exp(t/\tau_2)] \quad (10)$$

where $\tau_1 = 0.7 \pm 0.1$ ns, $\tau_2 = 7 \pm 0.5$ ns, $\beta_1/\beta_2 = 6.9 \pm 0.3$, and $\Delta\nu_f = \nu_e^0(0) - \nu_e^0(\infty)$.

So we can see that during the first stage of relaxation the spectra is shifting by an order of magnitude faster than at the end. Most of the spectral shift (about 66%) takes place during the first 3 ns. Temporal change of the rms deviation $\sigma(t)$ of the IBF is indicated by the points in Fig. 5b. As before, the value $\sigma(t=0)$ was determined from (9). Because of the insufficient temporal resolution of our setup, we could not find the exact value of $\sigma(t)$ in the time range 0–3 ns. Nevertheless, it may be concluded from the data obtained that during this period the half-width of the IBF grows, while at the later time period it falls exponentially with a characteristic time equal to $\tau_3 = 6.0 \pm 0.3$ ns. It follows from the above data that, when describing the fluorescence decay at any fixed wavelength, it is most important to take into consideration the fast spectral shift of the IBF maximum during the first stage of relaxation (the change of the IBF half-width at this period is less important) and the change of the IBF half-width at the later period (when the maximum is moving very slowly). So for calculation of the temporal behavior of fluorescence, we assumed that the maximum of the IBF is shifting in accordance with formula (10), while its half-width decreases exponentially with time constant τ_3 (solid curve in Fig. 5b). Figure 6 shows the calculated curves (1′,2′) and experimentally measured dependencies (1, 2) of fluorescence intensity on time for two wavelengths—one chosen at the blue slope of the fluorescence band (curves 1 and 1′) and another at the red slope (curves 2 and 2′). As we can see there is a very good agreement between calculated and experimental data.

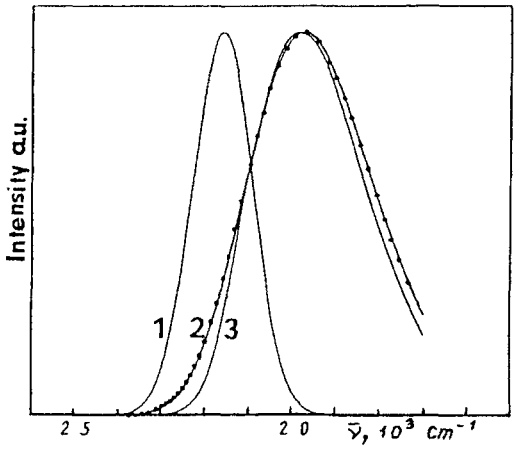

Fig. 3. An example of calculating the IBF for the fluorescence (1) from the time-resolved spectrum (2) of 3ANMP in glycerol at the moment 6 ns after onset of the excitation pulse and the homogeneous fluorescence spectrum of 3ANMP in hexane (3).

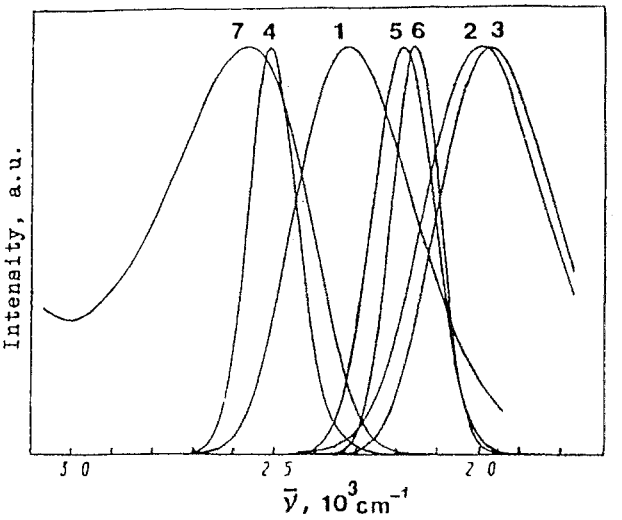

Fig. 4. 3ANMP in glycerol. Calculation of the time-resolved fluorescence spectrum (1) and IBF (4) at the zero instant of time. (2, 3) Experimental fluorescence spectra at times 3 and 16 ns after the onset of the excitation pulse; (5, 6) IBF determined from these spectra; (7) stationary absorption spectrum.

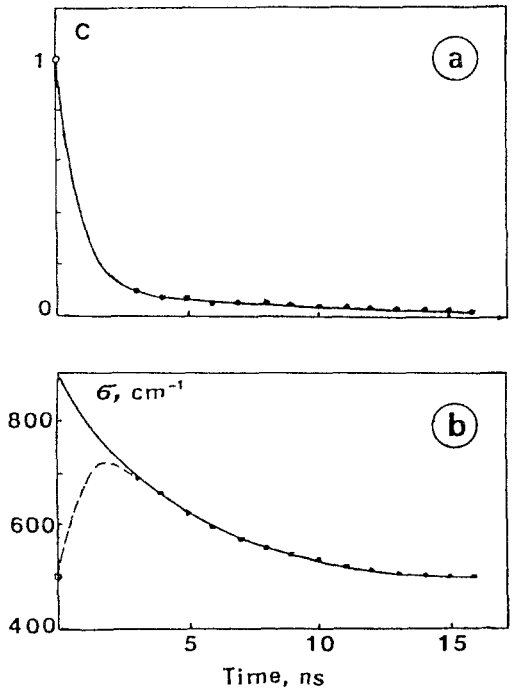

Fig. 5. (a) Correlation function $C(t) = [\nu_e^e(t) - \nu_e^e(0)]/[\nu_e^e(0) - \nu_e^e(\infty)]$. The points are calculated from maximum positions of IBF found for the excited state from experimental time-resolved spectra. As the time-resolved spectrum at 0 time, we used the spectrum calculated by the method described in the text. The solid line is the double-exponential approximation by Eq. (10). (b) The time dependence of the rms deviation of IBF. The points were determined from experimental time-resolved fluorescence spectra by the method described in the text. The value of $\sigma(0)$ was determined by the method described in the text. The solid line represents the calculation. The dashed line shows the expected true time dependence of the rms deviation of IBF.

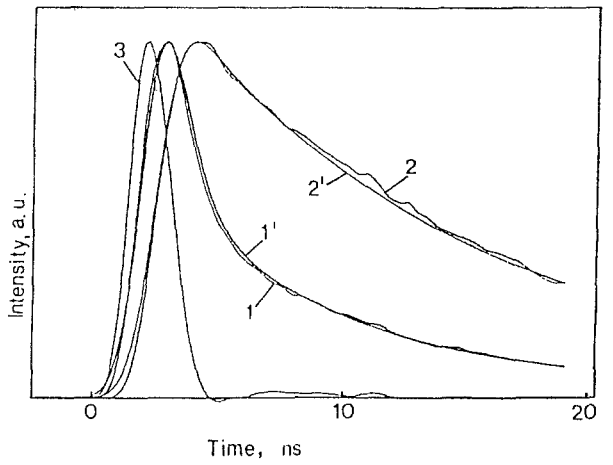

Fig. 6. Experimental (1, 2) and calculated (1′, 2′) fluorescence kinetics of 3ANMP solution in glycerol recorded on the blue (22,470 cm^{-1}) and red (18,350 cm^{-1}) slopes of the fluorescence spectrum, respectively. (3) Excitation pulse.

So the introduction of the function of inhomogeneous broadening into the theory of polar solutions proved to be quite efficient for the quantitative description of the spectral and temporal behavior of such systems after optical excitation. On the other hand, the correct description of the TDFS of polar solutions demands the knowledge of this function. From this point of view, the results presented in Fig. 5 are of special interest, as they are the first experimentally obtained data on the temporal evolution of IBF.

Rotational Dynamics

Experimental Results

Some experimental results of the investigation of the kinetics of fluorescence anisotropy of 3ANMP in glycerol at 28°C have been published in Ref. 25. Figures 7a and 8a give time-resolved fluorescence spectra at time instants 3 and 10 ns after the onset of excitation (curves 1 and 2) for two excitation frequencies: 25,600 and 20,800 cm^{-1}, which correspond to the frequencies ν_{ex}^1 and ν_{ex}^2 shown in Fig. 1. These two cases are of interest due to the fact that, in the first case, we deal with the red and, in the second case, with the blue shift of time-resolved spectra during relaxation. These figures also show the time-resolved value of anisotropy of the emission spectrum (time-resolved spectrum of emission anisotropy) for the same instant of time (curves 1′ and 2′). Curves 1″ and 2″ were obtained by the processing of experimental data with the least-squares technique (approximation by a polynomial of second degree).

These experimental data show that the time-resolved values of anisotropy monotonically change across the fluorescence band. The peculiar point is that the direction of this change depends on the excitation frequency (Figs. 7a and 8a, curves 1″ and 2″). In the first case (excitation of ν_{ex}^1), the time-resolved anisotropy is higher on the blue slope of curve, while in the second case (excitation of ν_{ex}^2), on the contrary, it is higher on the red slope. In other words, the degree of anisotropy happens to be always higher in the spectral region where the maximum contribution to the fluorescence is made by the solvate which has not yet experienced spectral relaxation. The experiment also showed that at the excitation of the solution by the specific frequency ν^*(21,700 cm^{-2}) when the spectral relaxation was absent, the an-

isotropy did not exhibit any dependence on the recording frequency.

In correlation with the data discussed above is the dependence of the fluorescence anisotropy kinetics on the registration frequency. Figures 7b and 8b show the anisotropy kinetics (curves 1 and 2) recorded on the blue and red slope of the fluorescence spectrum for ν_{ex}^1 and ν_{ex}^2 excitations. Curves 1′ and 2′ approximate the experimental data with the least-squares technique by a polynomial of the second degree. Curves 3 in Figs. 7b

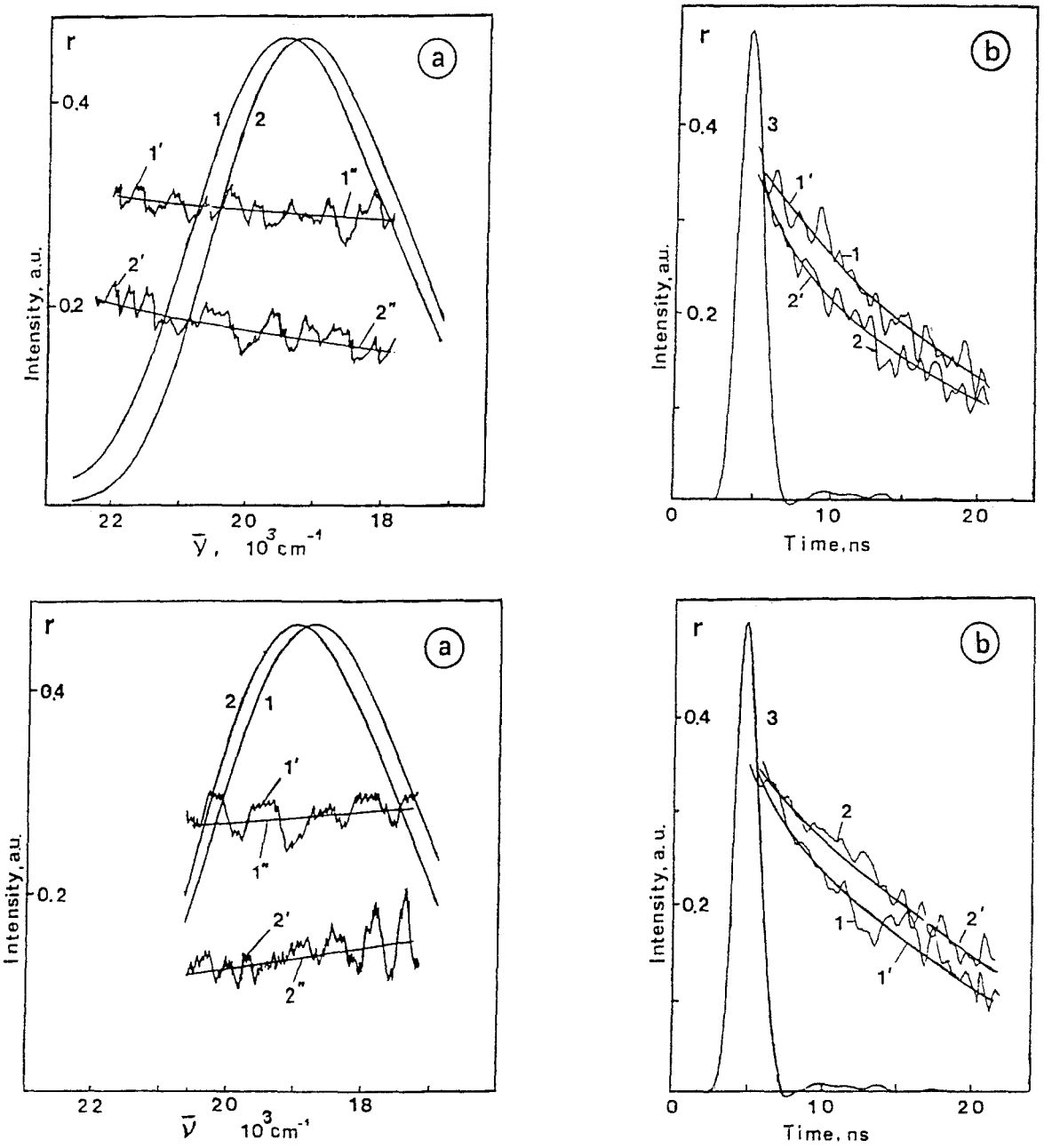

Figs. 7 and 8. The results of the investigation of fluorescence anisotropy at Stokes (25,600 cm^{-1}) and anti-Stokes (20,800 cm^{-1}) excitations. (a) 1 and 2—time-resolved fluorescence spectra at times 3 and 10 ns (Fig. 7) and 3 and 11 ns (Fig. 8) after the onset of the excitation pulse; 1′ and 2′—time-resolved spectra of emission anisotropy; 1″ and 2″—approximation of experimental data by a polynomial of second degree. (b) 1 and 2—anisotropy kinetics recorded on the blue and red slopes of fluorescence spectra (22,200 and 18,500 cm^{-1} for Fig. 7, 20,600 and 19,200 cm^{-1} for Fig. 8); 1′ and 2′—approximation of experimental data by a polynomial of second degree; 3—excitation pulse.

and 8 represent excitation pulses. It is seen from Fig. 7b that at Stokes excitation, the degree of anisotropy decreases faster on the red slope than on the blue one (curve 2'). Representation of curves 1' and 2' on a semilogarifmic scale shows that the anisotropy on the blue slope decays exponentially with the rotation time, 16 ± 1 ns. The decay of anisotropy on the red slope has a more complicated behavior. During the initial period (when relaxation of the solvate structure is going on), the decay goes faster, while in the later period the decay time corresponds to the same rotational diffusion constant as in the previous case, i.e., 16 ± 1 ns. In the case of ν_{ex}^2 excitation, the experiment gives opposite results. The exponential decay of anisotropy takes place on the red slope (Fig. 8b, curve 2) and the fast component is observed on the blue slope (curve 1). The rotational diffusion times on the red and blue slopes on completion of the spectral relaxation are approximately the same as in the first case of ν_{ex}^1 excitation. Thus, it is seen from the experiment that, in the general case, the fluorescence anisotropy kinetics recorded at a fixed frequency cannot be described by a single exponent and the relative contribution of the fast process is higher the greater the contribution to the fluorescence from the solvates which went through the spectral relaxation.

When analyzing the result of the rotational dynamics of the fluorofore, one may notice the correlation between the direction of the spectral relaxation and the character of the time-resolved spectra of fluorescence anisotropy. This correlation gives grounds for assuming that in the process of spectral relaxation, the fluorofore experiences additional rotation. The value of the additional depolarization caused by this rotation must depend on the quantity of the thermal energy released during the solvate relaxation.

The Thermal Regime of the Solvate

From the analysis of the field diagram [Eqs. (2) and (4)], one can find the relation between the free energy excess ΔF_e and the frequencies of excitation ν_{ex} and emission ν_{em}:

$$\Delta F_e = \text{Const}\,(\nu_{ex} - \nu_{em})(\nu_{ex} + \nu_{em} - 2\nu^*) \quad (11)$$

It follows from Eq. (11) that only in the one case where $\nu_{ex} = \nu^*$ does the spectral relaxation not take place. In this case $\nu_{em} = \nu^*$ and $\Delta F_e = 0$. In all other cases ($\nu_{ex} > \nu^*$ or $\nu_{em} < \nu^*$), the value $\Delta F > 0$. As the result of intermolecular relaxation, this free energy excess is converted to kinetic energy of motion of the solvate molecules. This can be thought of as if a heat source is functioning in the solvate. If the solution is excited at the absorption maximum, the amount of heat released in the excited solvate is equal to $\Delta Q = \Delta F_e = (h\Delta\nu_f/2)$. The coefficient 1/2 means that only half of the energy $h\Delta\nu_f$ is spent on heating up the excited solvent. The remaining part of the energy is released after transition of the chromofore to the ground state and does not affect fluorescence anisotropy kinetics (see the diagram in Fig. 1). Since $\beta_1/\beta_2 = 6.9$ [see formula (10)], the intensity of this source must be determined mostly by the first stage of spectral relaxation, which takes place at a rate of $1/\tau_1$. Omitting the second term in the right part of formula (10), we obtain the following expression for evolution of emission frequency ν_{em}:

$$\nu_{em}(t) = \cong \nu(\infty) + \Delta\nu_f \exp(-t/\tau_1) \quad (12)$$

Using (2), (4), and (12), we obtain $\Delta F_e(t) = (h\Delta\nu_f/2)\exp(-2t/\tau_1)$. Then the heat source intensity, which is determined by the time derivative of $\Delta F_e(t)$, will be given as follows: $(2\Delta Q/\tau_T)\exp(-2/\tau_1)$. Now we can write the equation describing the change in the quantity of heat in the solvate during the relaxation process:

$$Q(t) = Q_o + \delta Q(t) \quad (13)$$

Here Q_o is the heat quantity in the equilibrium solvate, and the function $\delta Q(t)$ can be determined from the balance equation of heat:

$$\frac{d}{dt}(\delta Q(t)) = \frac{2\Delta Q}{\tau_1}\exp(-2/\tau_1) - \frac{1}{\tau_T}\delta Q(t) \quad (14)$$

where τ_T is the heat relaxation time of the solvate. The solution of Eq. (14) has the following form:

$$\delta Q(t) = \frac{\Delta Q}{(\tau_1/2\tau_T) - 1}[\exp(-2t/\tau_1) - \exp(-t/\tau_T)] \quad (15)$$

It follows from Eq. (15) that the thermal regime of the solvate is determined by the ratio of the times τ_1 and τ_T. The heat relaxation time can be estimated using the relation known from the thermodynamics [38]:

$$\tau_T = \frac{\rho_d C_{P_L} VL}{\lambda S} \quad (16)$$

where ρ_d is the solvent density, C_{F_L} is the heat capacity of the solvent determined under constant pressure, L is the average linear size of the cooling region, S and V are, respectively, the area of its surface and the volume, and λ is the thermal conductivity of the solvent.

Although the size of the solvate is not known exactly, we can estimate by formula (16) that the heat relaxation time amounts to picoseconds, i.e., $\tau_T << \tau_1$. Then from formulas (13) and (15), we can find the law

of temperature change in the solvate for $t > \tau_T$:

$$T(t) = T_o + \Delta T \exp(-2t/\tau_1) \quad (17)$$

where T_o is the equilibrium solvate temperature and C^{solv} is its heat capacity.

The value of ΔT_o can be determined by experiment. Indeed, if the temperature is time dependent, the rotational diffusion time will be time dependent too:

$$\tau_{rot}(t) = [V\eta(T)/(kT(t)] \quad (18)$$

[The variation of the glycerol dynamic viscosity with temperature was taken from Ref. 39: $\lg\eta(cP) = A' + B'/(T-T')$; $A' = -2.8834$, $B' = 997.86$, $T' = 128.481°K$.]

As shown in Ref. 24, the emission anisotropy kinetics for the case of variable times of rotational diffusion is given by the following expression:

$$r(t) = r_o \exp\left[-\int_o^t dt'/\tau_{rot}(t')\right] \quad (19)$$

where r_o is the limiting value of anisotropy. The results of calculation of the anisotropy kinetics by formula (19) taking into account (18) for temperature ΔT varied from 30 to 70°C are presented in Fig. 9. Formula (19) gives the anisotropy kinetics in the solvate in which spectral relaxation takes place. For correct experimental verification of this formula, it would be necessary to follow the same type of solvates in the process of their spectral relaxation, i.e., we would be obligated to shift the recording frequency synchronously with the time-resolved spectrum shift. Moreover, we ought to bear in mind that the homogeneous contour of fluorescence of an individual solvate has a significant width. Due to this fact the contribution of the measured anisotropy at any fixed wavelength is made by solvates which happen to be at different stages of spectral relaxation. So it will not be correct to compare our calculated curves (Fig. 9) with experiment (curves 1″ and 2″; Fig. 7b). An attempt to take into account the points discussed above is made in the next section. It is shown here that the value of the depolarization caused by the spectral relaxation must be about 0.1. Then we can find from Fig. 9 that the value of ΔT in formula (16) is expected to be 50 ± 5°C.

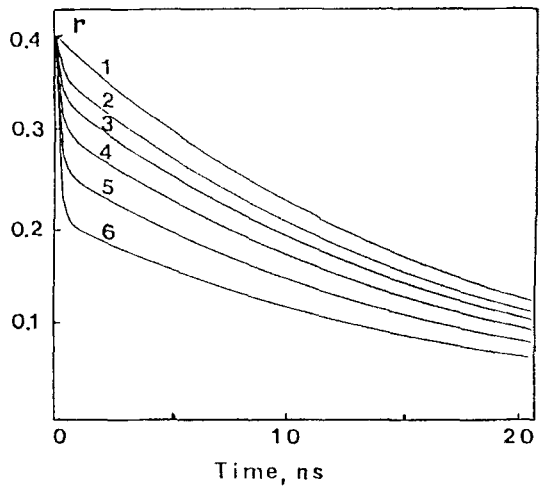

Fig. 9. The kinetics of emission anisotropy calculated by the model taking into account the solvate temperature variation during spectral relaxation [ΔT are 30°C (2), 40°C (3), 50°C (4), 60°C (5), and 70°C (6)] and by Levshin-Perrine theory (curve 1, T_o = 20°C).

If we assume that the solvate has the form of a sphere, we can find from (16) that

$$\tau_T = C^{solv}/(2\pi R^{solv}\lambda) \quad (20)$$

where R^{solv} is the solvate radius. Then from (15), (17), and (20), we have

$$\Delta T = \frac{h\Delta\nu_f 2\tau_T}{2C^{solv}\tau_1} = \frac{h\Delta\nu_f}{2\pi R^{solv}\lambda\tau_1} \quad (21)$$

Now from formula (21) we can determine the solvate radius. At $\Delta T = 50°C$ it turned out to be equal to R^{solv} = 9.4 Å. Knowing the size of 3ANMP and glycerol molecules, we can estimate the number of molecules entering into the solvate. For the process of equilibrium Brownian diffusion, we can find by the Einstein relation that R_{3ANMP} = 2.88 Å. According to Ref. 40 the glycerol molecule radius is estimated to be about 3 Å. Then, from geometrical considerations, it follows that the solvate is formed by 19 molecules including the chromofore molecule; i.e., it represents a chromofore surrounded by one layer of glycerol molecules.

The Spectral Dependence of the Instantaneous Value of Emission Anisotropy

The description of the anisotropy kinetics without taking into account the distribution of solvates over the frequencies of pure electronic transition fails to explain the spectral dependence of time-resolved value of fluorescence anisotropy. But in reality the time-resolved spectrum is not homogeneous, and during relaxation not only is the center of gravity of the inhomogeneous broadening function shifted, but also its width changes.

To simplify the analysis of the influence of inhomogeneous broadening of solvates on the spectral dependence of time-resolved values of the anisotropy, we employ the following model. Let us assume that instead of the

continuous distribution over the frequencies of pure electronic transition, we have only two types of centers: nonequilibrium and equilibrium. In this case the emission anisotropy is given the following relation:

$$r(\nu,t) = \sum_{i=1}^{2} r_i(t)\, f_i(\nu,t) \qquad (22)$$

where $r_1(t) = r_o \exp(-t/\tau_{rot})$ is the time-dependent anisotropy of the nonequilibrium solvate and $r_2(t) = (r_o - \Delta r)\exp(-t/\tau_{rot})$ is the similar value for the equilibrium solvate. The value Δr is a fluorescence depolarization due to wavelength-dependent rotation of dye molecules; the value of $f_i(\nu,t)$ describes the contribution of each state to the total fluorescence:

$$f_i(\nu,t) = \frac{I_i(\nu,t)}{I_\Sigma(\nu,t)} \qquad (23)$$

where $I_i(\nu,t)$ is the fluorescence of individual states and $I_\Sigma(\nu,t)$ is their total fluorescence. For calculation by formula (22) it is necessary to know the fluorescence spectra of these two states, their lifetimes, and the relaxation time. In calculations we used, as the non-equilibrium-state spectrum, the fluorescence spectrum of this chromofore in hexane and, as the equilibrium-state spectrum, the time-resolved fluorescence spectrum, measured on completion of spectral relaxation. All time constants required for calculation were determined by experiment. It turned out that the best agreement between time-resolved anisotropy spectra calculated by formula (22) and measured experimentally and approximated by least-squares technique (curves 1″ and 2″; Fig. 7a) were attained at $\Delta r = 0.1 \pm 0.02$. Using this value and the Levshin-Perrine formula for limiting values of anisotropy $r_{lim} = 0.2(3\cos^2\xi - 1)$ [ξ is the angle between the absorption and the emission oscillator and $r_{lim} = (0.4 - \Delta r)$], we found an additional angle at which molecules of 3ANMP in glycerol turn off light-induced rotation. At ν^1_{ex} excitation (25,600 cm^{-1}) its value turned out to be equal to 24 ± 3°.

It should be noted that our data on the kinetics of fluorescence depolarization (Figs. 7 and 8) cannot be explained by the mechanism proposed in Ref. 24. Indeed, if the fluorescence depolarization was hindered with time due to the enhancement of the chromofore–environment interaction or to the H-bond formation, we may expect the following effect. The speed of depolarization of fluorescence in the case when its maximum moves toward the long waves should be lower at the red slope of the fluorescence band than at the blue slope. As demonstrated above our experiments showed the opposite effect.

The authors of Ref. 13 assumed, for describing the abnormal rotation of coumarin-153 in a polar solution, that during spectral relaxation the rotation of the emission dipole moment can take place due to the change in the solvate configuration. This assumption is substantiated by the fact that the fluorescence spectrum width of this molecule in a nonpolar solution is greater than in a polar solution and that the fluorescence spectrum loses the vibrational structure as one passes from nonpolar solutions. Such a mechanism can probably take place in some molecular systems. However, for 3ANMP no reduction of the fluorescence spectrum width is observed with increases in solvent polarity. Besides, we managed to describe the fluorescence kinetics under the assumption that the homogeneous spectrum remains unaffected in the process of spectral relaxation. For this spectrum, we used that of fluorescence in the nonpolar solvent. It is probable that the weak sensitivity of the S_1 state to the environment polarization for the 3ANMP molecule is explained by the fact that in this molecule an intramolecular H bond is formed which fixes the position of the amino group [41,42].

It is also clear that nonexponential kinetics of fluorescence anisotropy is not associated with the form of the 3ANMP molecule, since the hydrodynamic theory for such molecules predicts a much weaker nonexponentially [20] which, in addition, must depend neither on the excitation nor on the detection frequency.

CONCLUSION

Analysis of the experimental and theoretical results has revealed the following. The kinetics of anisotropy of 3ANMP in glycerol depends on the excitation and detection frequency and, in the general case, is not exponential. Besides the equilibrium Brownian diffusion, there exists a faster process (wavelength dependent), which takes place during spectral relaxation. Its role in fluorescence depolarization at a given frequency is more important the greater the contribution made to fluorescence at this frequency by the solvates which have undergone spectral relaxation and the higher the IBF deviation from equilibrium at the initial moment after optical excitation.

The wavelength-dependent rotation can be expected for any molecule in a polar solution if, after optical excitation, there is a change in the value of the constant electrical dipole moment, its direction, or both. The effect must be greater the stronger the heating up of the solvate is in the process of relaxation and the longer the action of the heat source lasts.

The equilibrium IBF for absorption and emission

has a Gaussian shape, and its width in the ground state is greater than in the excited state. The nonequilibrium IBF for fluorescence, within experimental accuracy, can also be considered as Gaussian during the whole period of relaxation, beginning from 3 ns after excitation. The relaxation of the IBF center of gravity to its equilibrium position may be described by two exponents. At the initial stage the spectral shift occurs by an order of magnitude faster than at the end of relaxation. The complicated character of the spectrum shift indicates that the Debye model cannot be used for describing the dielectric properties of glycerol.

The account of the distribution of solvates over the frequencies of pure electronic transition makes it possible to describe fully the kinetics of the fluorescence and TDFS by the evolution of the inhomogeneous broadening function.

REFERENCES

1. A. P. Demchenko (1986) *Ultraviolet Spectroscopy of Proteins*, Springer-Verlag, Berlin.
2. D. F. Calef and G. P. Wolynes (1983) *J. Phys. Chem.* **78**, 4145.
3. S. G. Su and J. D. Simon (1988) *J. Chem. Phys.* **89**, 908.
4. H. Sumi and R. A. Marcus (1986) *Chem. Phys. Lett.* **84**, 4272.
5. I. Rips, J. Klafter, and J. Jortner (1988) *J. Chem. Phys.* **88**, 3246.
6. A. N. Rubinov and V. I. Tomin (1970) *Opt. Spectr. (USSR)* **29**, 1082.
7. Yu. T. Mazurenko and N. G. Bakhshiev (1970) *Opt. Spectr. (USSR)* **28**, 905.
8. N. G. Bakhshiev (1972) *Spectroscopy of Intermolecular Interactions*, Nauka, Leningrad.
9. Yu. T. Mazurenko (1974) *Opt. Spectr. (USSR)* **36**, 905.
10. G. van der Zwan and J. T. Hyneš (1985) *J. Phys. Chem.* **89**, 4181.
11. B. Bagchi, D. W. Oxtobi, and G. R. Fleming (1984) *Chem. Phys.* **8**, 257.
12. E. W. Castner, B. Bagchi, M. Maroncelli, S. P. Webb, A. J. Ruggiero, and G. R. Fleming (1988) *Ber. Bunsenges. Phys. Chem.* **92**, 363.
13. M. Maroncelli and G. R. Fleming (1987) *J. Chem. Phys.* **86**, 6221.
14. P. J. Stiles and J. B. Hubbard (1984) *Chem. Phys.* **84**, 431.
15. P. Madden and D. Kivelson (1982) *J. Phys. Chem.* **86**, 4244.
16. P. G. Wolynes (1987) *J. Chem. Phys.* **86**, 5133.
17. R. F. Loring and S. Mukamel (1987) *J. Chem. Phys.* **87**, 1272.
18. R. P. DeToma, J. H. Easter, and L. Brand (1976) *J. Am. Chem. Soc.* **98**, 5001.
19. V. T. Koyava, A. M. Sarzhevsky, and V. G. Sharonov (1981) *J. Prikl. Spectr. (USSR)* **41**, 580.
20. V. A. Gaisyonok and A. M. Sarzhevsky (1986) *Absorption and Luminescence Anisotropy of Polyatomic Molecules*, Universitetskoe, Minsk.
21. Yu. L. Klimontovich (1983) *Statistical Physics*, Nauka, Moscow.
22. D. M. Gakamsky, N. A. Nemkovich, A. N. Rubinov, and V. I. Tomin (1983), *Opt. Spectrosc. (USSR)* **54**, 567.
23. Yu. T. Mazurenko, N. G. Bakhshiev, and I. V. Piterskaya (1968) *Opt. Spectr. (USSR)* **25**, 92.
24. J. R. Lakowicz (1984) *Biophys. Chem.* **19**, 13.
25. D. M. Gakamsky, N. A. Nemkovich, A. N. Rubinov, and V. I. Tomin, (1988) *Opt. Spectr. (USSR)* **64**, 678.
26. L. E. Fried and S. Mukamel (1990) *J. Chem. Phys.* **93**, 932.
27. A. L. Nichols III and D. F. Calef (1988) *J. Chem. Phys.* **89**, 3783.
28. N. A. Nemkovich, A. N. Rubinov, and V. I. Tomin (1991) in J. R. Lakowicz (Ed.), *Topics in Fluorescence Spectroscopy, Vol. 2. Principles*, Plenum Press, New York, Chap. 8.
29. N. A. Nemkovich, V. I. Matseiko, A. N. Rubinov, and V. I. Tomin (1979) *Pisma Zh. Eksper. Teor. Fiz. (USSR)* **12**, 780. N. A. Nemkovich, V. I. Matseiko, and V. I. Tomin (1980) *Opt. Spectr. (USSR)* **49**, 274.
30. D. M. Gakamsky, N. A. Nemkovich, A. N. Rubinov, V. I. Tomin, and E. V. Chaikovsky (1986) *Kvant. Elektr. (USSR)* **13**, 2271.
31. A. D. Stein and M. D. Fayer (1991) *Chem. Phys. Lett.* **176**, 159.
32. A. D. Stein, K. A. Peterson, and M. D. Fayer (1989) *Chem. Phys. Lett.* **161**, 16.
33. A. D. Stein, K. A. Peterson, and M. D. Fayer (1990) *J. Chem. Phys.* **92**, 5622.
34. N. A. Nemkovich, A. N. Rubinov, and V. I. Tomin (1981) *J. Lumin.* **23**, 349.
35. A. N. Rubinov, E. I. Zenkevich, N. A. Nemkovich, and V. I. Tomin (1982) *J. Lumin.* **26**, 367.
36. Yu. T. Mazurenko (1980) *Opt. Spectr. (USSR)* **48**, 704.
37. B. I. Stepanov (1958) *Izv. Akad. Nauk SSSR (USSR)* **22**, 1367.
38. A. N. Matveyev (1987) *Molecular Physics*, Vysshaya shcola, Moscow.
39. R. C. Reid, J. M. Prausnitz, and T. K. Sherwood (1982) *The Properties of Gases and Liquids*, Chimiya, Leningrad.
40. N. F. Zhevandrov and V. P. Nicolayev (1957) *Doklady Akad. Nauk SSSR (USSR)* **133**, 1025.
41. J. Szadowski (1981) *Dyes and Pigments* **2**, 249.
42. D. Noukakis and P. Suppan. (1991) *J. Lumin.* **47**, 285.